International Journal Of Engineering Research And Development
e- ISSN: 2278-067X, p-ISSN: 2278-800X, www.ijerd.com
Volume 14, Issue 9 (September Ver. I 2018), PP.43-49

Structural and optical properties of TiO_2 and TiO_2-Zeolites composites films

*K. M. Álvarez[1], J. J. Alvarado[1], B. S. Soto[1] and M. A. Hernandez[2]
[1]*Centro de Investigación en DispositivosSemiconductores, Benemerita Universidad Autonoma de Puebla, Puebla, 72570, México.*
[2]*Departmento de Investigación en Zeolitas, Benemerita Universidad Autonoma de Puebla, Puebla, 72570, Puebla, México.*
Corresponding Author: K. M. Álvarez

ABSTRACT*Thin films of TiO_2 and TiO_2-Zeolite were deposited with different concentrations on glass substrates using the spin-coating technique. X-ray diffraction (XRD), UV-vis, Raman spectroscopy and scanning electron microscopy (SEM) characterizations were used in order to determine the influence of this variation on the structural, optical and morphological properties of the films. As a result, it was found that the films are polycrystals, an exhibit high transmittance in the visible and near infrared regions. Furthermore, the narrow optical bands are in the range of 4.03 eV-4.46eV, and the morphology of the samples shows conglomerates with sizes less than 10 μm.*

KEYWORDS*: Titanium oxide, Zeolite, Optical properties, Sol-gel and Thin Film.*

Date of Submission: 03-11-2018 Date of acceptance: 17-11-2018

I. INTRODUCTION

Since the research of photocatalytic water split on TiO_2 electrodes was conducted in 1972, the photocatalytic oxidation of aqueous and gaseous contaminants has been extensively studied [1].However, the widespread use of TiO_2 has been restricted because of its some drawbacks including low adsorption capacity. Therefore, many studies have been focused on supporting TiO_2 nanoparticles on certain matrix [2]. Some of the matrices that we can find in the literature are active carbon [3], glass [4], grapheme [5] and zeolite [6]. Furthermore, TiO_2 has been attracted extensive attention due to higher stability, cheapness and activity photocatalytic []. Adsorption-photocatalyst hybrids (AHP's) are bifunctional materials based on an adsorbent and a photocatalyst with great potential for decontamination processes [8].

Zeolites are crystalline microporousaluminosilicates that are widely used as adsorbents and catalysts [8], these materials display a number of unique properties such as: a presence of strong acidic centers, large specific surface area, high ion-exchange ability, high thermal stability, precisely defined system of micropores and channels which enable conducting shape-selective catalytic reactions [10]. Thanks to these properties, Zeolites can be then applied in catalysis.

According to the International Union of Pure and Applied Chemistry (IUPAC) the zeolites can be classified in three groups; micropores (> 2nm), mesopoross (2-50nm) and macropores (<50 nm) [11], within micropore materials we can find Erionite [12], Mordenite [13] and Clinoptilolite [14].

Although TiO_2-Zeolite powders have been previously studied [13] which have shown incredible optical properties. This work aims to demonstrate that it is possible to incorporate TiO_2 in Zeolites to make films, the zeolites used were: Erionite, Mordenite and Clinoptilolite, since they have small pores in which small molecules can be captured (dimethylether, CO_2, etc.) and can be incorporated to these materials, which can be used in the future as photocatalysts.

II. MATERIAL AND METHODS

2.1 Material and methods

2.1.1.Chemical Compounds

Titanium isopropoxide(Sigma-Aldrich, Cas N° 546-68-9), isopropanol (J.T. Baker, Cas N° 67-63-0) and ammonium hydroxide (EM SCIENCE, Cas N° 1336-21-6).

2.1.2.Synthesis of TiO_2 nanoparticle

TiO_2 films and the TiO_2-Zeolite compounds were obtained by the sol-gel method, which consisted in the following:

i) Mixing: the precursor titanium isopropoxide was mixed with the solvent isopropanol.
ii) Gelification: Sodium hydroxide was added to generate the gelation.

iii) Aging: it consisted of allowing the sample to stand for about 24 hours
iv) Drying: the temperature used in this stage was 80 ° C in order to remove the solvent and the organic components for a time of approximately 6 hrs.
v) Sintering: The nanoparticles were left at a temperature of 500 ° C for an approximate time of 1 hr for the restructuring of their networks.

2.2.Synthesis of TiO_2 nanocomposite

In the case of the composites of TiO_2 with Zeolites, they are carried out in situ, which means that we add the natural Zeolites in the mixing stage of the TiO_2process.In the present work, 9 samples were made as shown in Table 1.

Table 1: Weight % by of the films of the composites.

Sample	% weight of TiO_2	% weight of Zeolite	% Total
$TiO_2 - Eri\ (75-25)$	75.00	25.00	100.00
$TiO_2 - Eri\ (50-50)$	50.00	50.00	100.00
$TiO_2 - Eri\ (25-75)$	25.00	75.00	100.00
$TiO_2 - Cli\ (75-25)$	75.00	25.00	100.00
$TiO_2 - Cli\ (50-50)$	50.00	50.00	100.00
$TiO_2 - Cli\ (25-75)$	25.00	75.00	100.00
$TiO_2 - Mor\ (75-25)$	75.00	25.00	100.00
$TiO_2 - Mor(50-50)$	50.00	50.00	100.00
$TiO_2 - Mor\ (25-75)$	25.00	75.00	100.00

2.1.3 **Deposition of films by the Sol-Gel method**

The nanoparticles of TiO_2 and TiO_2-Zeolites were redispersed in methanol and subsequently deposited by the spin-coating method at 1000 rpm.

III. RESULTS AND DISCUSSION

Figure 1a shows diffraction patterns of the films of the TiO_2-Erionite composites in their different concentrations. The XRD spectra shows a good crystallization of the samples and the presence of the anatase phase (peak attributed to 2θ = 25,281° of the plane (101)) with the reference 00-021-1272 (ICCD, 2015) corresponds to composites with phase anatase. Moreover, in the case of the sample that has a high content of Erionite, the peak attributed to 2θ = 31.46° is observed in the plane (214) with the reference 00-088-1223 (ICCD, 2015) [15-16].

Furthermore, considering the films with TiO_2-Clinoptilolite, the presence of the anatase phase can also be observed thanks to the peak located at 2θ = 25.281° of the plane (101). If the amount of clinoptilolite increases, it is possible to observe a peak located at 2θ = 31.322° of the plane (-242) with reference 04-016-1257 (ICCD, 2015), which corresponds to the Clinoptilolite sample [15].

Additionally, for the TiO_2-Mordenite films, the peak located at 2θ = 25.281° of the plane (101) corresponding to the anatase phase of TiO_2 is observed, while as the amount of zeolite mordenite increases, the peaks located at 2θ = 22.206°, 23.144°, 24.572°, 26,268°, 27,681° and 30,851° of the plans (150), (241), (510), (350), (511) and (332) with reference 029-1790 (ICCD, 2015) appears [15].

Previous research has shown that these composites have several orientations due to the mixture of anatase and zeolite (Erionite, Clinoptilolite and Mordenite). However when they are deposited by spin coating the amount of orientations decreases. According to Mishra et al., the surface energies, play a key role in the determination of the grain growth in certain orientation [15-17], they also have carried out studies on the calculation of surface energy to know the growth of the grain in certain orientations.

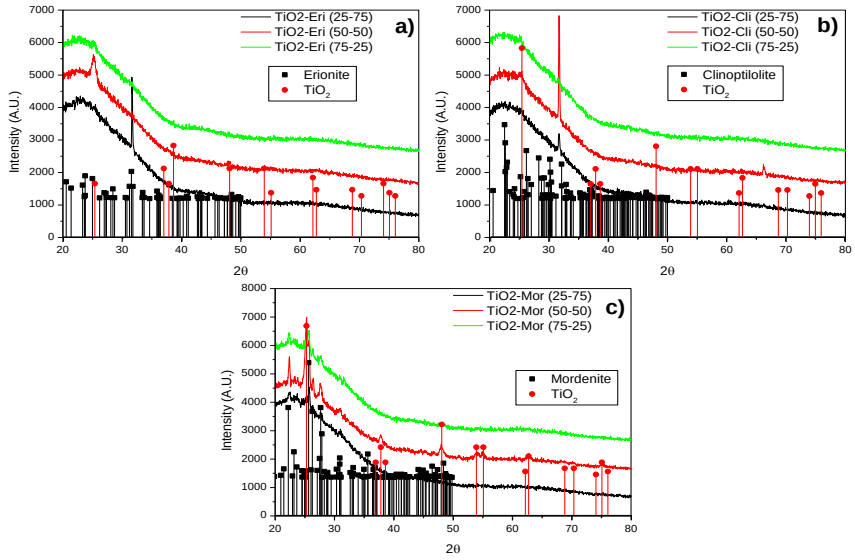

Figure 1: X-ray diffraction spectra of a) TiO_2-Erionite, b) TiO_2-Clinoptilolite and c) TiO_2-Mordenite.

3.2 Characterization by Retro-disperse Energy Spectroscopy (EDS).

Table 2 shows the elemental composition of the TiO_2-Zeolite composites, the presence of Ti and O is observed, which are elements related to TiO_2. However, the Al element is also related to alumosilicates (Al and Si) belonging to the zeolites, as well as successively some salts related to the different structures of the zeolites such as (Na, Mg, Si and Cl).

In the case of the samples with TiO_2-Erionite, it is observed that when its concentration has 75% of TiO_2 and 25% of Erionite, the Ti and O elements increase and when it presents 25% TiO2 and 75% Erionite these elements have a decrease, while the alumosilicates (Al and Si) increases along with the salts (Mg, Nay Cl), and Ca element is also present but this is due to the glass substrate in which the films were deposited.

On the other hand, the composites that have TiO_2-Cli, present a variation of the elements due to the higher content it has, that is, if it has a higher amount of TiO_2, its present elements (Ti and O) generate an increase in % W and a decrease in the content of alumosilicates (Al and Si) and salts (Na and Mg) as well as samples of TiO_2-Erionite this also shows Ca due to the substrate.

The study of the samples of TiO_2-Mordenite shows the dependence of the increase of TiO_2 (75%) and decrease of the Mordenite (25%), and this is achieved through the decrease of the alumosilicates (Al and Si) and the salts (Na, Mg, Cl and Ca) of the samples as well as their increase of Ti and O, these samples contain Calcium because the Mordenite reports salts of Calcium in its structure however it is also due to the substrate in which finds the film deposited.

In general, from these characterization it is observed how the presence of elements in the films increases or decreases according to the concentration they have contain in the material.

Table 2: Weight % and atomic % of the composites films.

Composites	% weight concentration in the synthesis	Element	Weight %	Atomic %
$TiO_2 - Eri\ (25-75)$	25% TiO_2	O	22.13	36.35
	75% Erionite	Na	15.54	15.00
		Mg	5.72	5.44
		Al	3.82	3.52
		Si	38.86	31.85
		Cl	3.12	2.35
		Ca	6.50	3.90
		Ti	4.31	1.59
		Total	**100.00**	**100.00**
$TiO_2 - Eri\ (75-25)$	75% TiO_2	O	37.97	52.19
	25% Erionite	Na	12.42	11.88
		Mg	2.86	2.58
		Al	1.59	1.29
		Si	32.32	25.31
		Cl	2.04	1.27

		Ca	5.77	3.17
		Ti	5.03	2.31
		Total	**100.00**	**100.00**
$TiO_2 - Cli\ (25-75)$	25% TiO_2 75% Clinoptilolite	O	35.64	58.39
		Na	9.65	8.16
		Mg	3.42	1.72
		Al	6.95	1.73
		Si	37.78	26.73
		Ca	3.89	1.82
		Ti	2.67	1.44
		Total	**100.00**	**100.00**
$TiO_2 - Cli\ (75-25)$	75% TiO_2 25% Clinoptilolite	O	44.42	56.83
		Na	8.92	7.84
		Mg	1.99	1.63
		Al	2.22	1.90
		Si	35.7	38.12
		Ca	3.46	1.72
		Ti	3.28	1.95
		Total	**100.00**	**100.00**
$TiO_2 - Mor\ (25-75)$	25% TiO_2 75% Mordenite	O	28.97	54.24
		Na	13.40	12.10
		Mg	3.62	2.55
		Al	2.16	1.19
		Si	38.3	25.17
		Cl	2.74	1.48
		Ca	6.88	3.17
		Ti	3.93	2.10
		Total	**100.00**	**100.00**
$TiO_2 - Mor\ (75-25)$	75% TiO_2 25% Mordenite	O	38.07	54.24
		Na	12.67	12.10
		Mg	2.82	2.55
		Al	1.46	1.19
		Si	32.21	25.17
		Cl	2.40	1.48
		Ca	5.79	3.17
		Ti	4.58	2.10
		Total	**100.00**	100.00

3.3 Raman

Figure 2 shows the Raman spectra of the TiO_2-Zeolite composites films, Figure 2 a) shows the TiO_2-Erionite composites, where two peaks are observed, which are related with the vibrational modes of TiO_2anatase phase located at 143 (Symmetrical O-Ti-O stretch) and 181 (Symmetrical O-Ti-O stretch). It is also observed that for the sample that has higher TiO_2 content, these peaks are very remarkable compared to those that have more Erionite (Zeolite), which is due to the vibrations that are strong in Raman if the bond is covalent, whereas are strong in IR if the bond is ionic [15,18].

In addition, the films of the TiO_2-Clinoptilolite composites are observed in Figure 2 b) where, like the TiO_2-Erionite films, it is possible to appreciate two vibrational modes allocated in 143 nm and 181 nm related to TiO_2 (this occurs with greater intensity to those that have higher TiO_2 content).

Figure 2 c) belongs to the samples of TiO_2-Mordenite, where it cannot be possible to distinguished any bands, this is because they show characteristic shot noises of the fluorescence due to the calcite ($CaCO_3$) present in the samples [15].

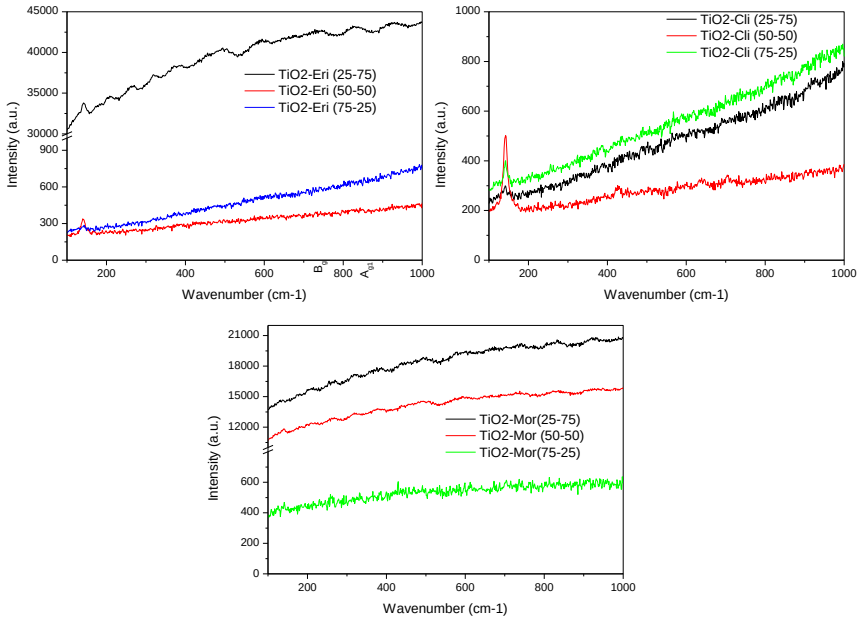

Figure 2: Raman Spectroscopy of a) TiO_2, b) TiO_2-Erionite, c) TiO_2-Clinoptilolite and d) TiO_2Mordenite.

3.4 UV-Vis

Diffuse reflection spectrum of the samples under study were recorded at room temperature, by employing Kubelka–Munk theory by using the formula: $F(R) = (1\text{-}R)^2/2R$, where R is the diffuse reflection factor and F(R) is the Kubelka-Munk function [19]. By using the Tauc algorithm, the optical band gap can be obtained $(F(R) * hV)^n$ [20].

This equation against hV is plotted and n= 0.5 (direct band gap) and 2 (indirect band gap). On the Tauc plot, a linear region just above the optical absorption edge is fitted and extrapolated to photon energy axis which is possible to observed in Figure 3 [15].

Finally, the optical band gap is obtained from the plot of the Tauc equation, whereby the intersection of the tangent to the turning point with the x-axis is use for the determination [20].

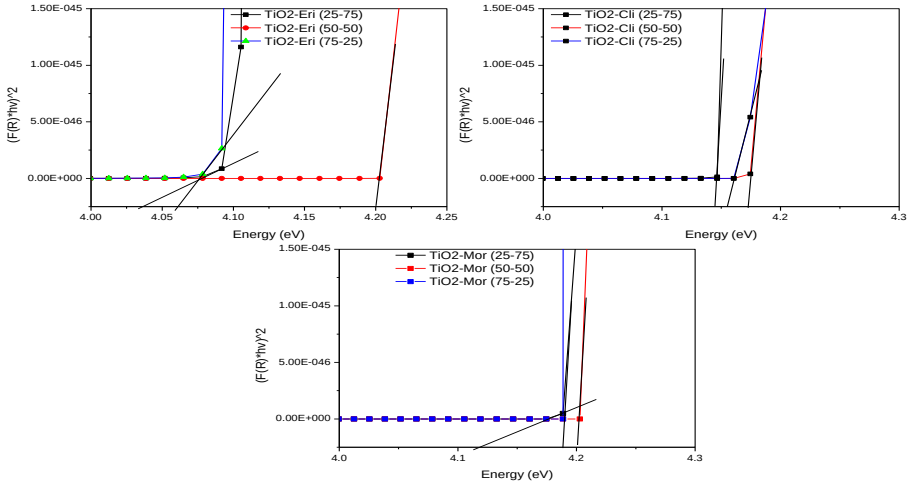

Figure 3: Band gap diagram of the different TiO_2-Zeolite composites films.

Table 3 shows the energies of the different compounds obtained by the Kubelka-Munk equation. Where the values obtained for these composites films are in the range of 4.05eV-4.46eV. It is observed that, when adding zeolite to TiO_2, a modification of the band gap is present, which generates an increase of the

bandgap. It is well known that this band interval belongs to the uv-vis region, which is important because photoexcitation occurs in this energy to generate photocatalysis. Previous studies have shown that this type of composite has a band interval less than 4 eV [13].The increase in this case is due to the presence of preferential orientations (monocrystals) that are presented in the film differences of powders that appear in more than one orientation (polycrystals) and that are related to conductivity [15-21]

Table 3: Different composites Band Gap.

Sample	Energy (eV)
$TiO_2 - Eri\ (75-25)$	4.02
$TiO_2 - Eri\ (50-50)$	4.03
$TiO_2 - Eri\ (25-75)$	4.05
$TiO_2 - Cli\ (75-25)$	4.43
$TiO_2 - Cli\ (50-50)$	4.44
$TiO_2 - Cli\ (25-75)$	4.46
$TiO_2 - Mor\ (75-25)$	4.20
$TiO_2 - Mor(50-50)$	4.27
$TiO_2 - Mor\ (25-75)$	4.33

3.5 Scanning Electronic Microscopy (SEM)

Figure 4 shows the different micrographs of the films of TiO_2-Zeolite composites. In Figures 4 a-d, we can see the films of the TiO_2-Eri (25-75) and TiO_2-Eri (75-25) composites, these films have a greater number of blocks and conglomerates when there is a greater amount of Erionite (75%) as seen in Figure 4 d), a difference when the amount of Erionite (25%) decreases as achieved in Figure 4 a), where the amounts of particles are small and there are also minute amounts of particles corresponding to TiO_2.

The films of the TiO_2-Cli composites are observed in Figures 4b-4e, in Figure 4b they are observed in the TiO_2-Cli composition (25-75), and in which a group of conglomerates can be identified in a zone. This is due to a type of deposit that was used (spin coating), which consists in the deposition of the layers by means of the drip in the central part of the substrate, which generates the greatest amount remains in the middle of the substrate that the layer is not homogeneous, another reason is the high content of zeolite in this sample that generates more conglomerates of a larger size, that the zeolite has large quantities, however, in Figure 4e corresponding to the sample TiO_2-Cli (75 -25) a better uniformity in the film is seen, this is due to a greater amount of nanoparticles of TiO_2 than of Zeolites which have a larger size than a large part of the TiO_2, that is why it disperses in a better way.

When we observed the Figures 4 c) and 4 f), which belongs to TiO_2-Mor (25-75) and TiO_2-Mor (75-25), the content of the Mordenite Zeolite is more clearly obtained, that is, in Figure 4 c) that has a smaller amount of Clinoptilolite, there are small and medium sized particles dissected on the surface of the substrate, while the sample that contains more percentage of Clinoptilolite (75%) is able to observe small particle sizes in very small quantity, but more information than the medium and large sizes of these particles belonging to the Clinoptilolite Zeolite.

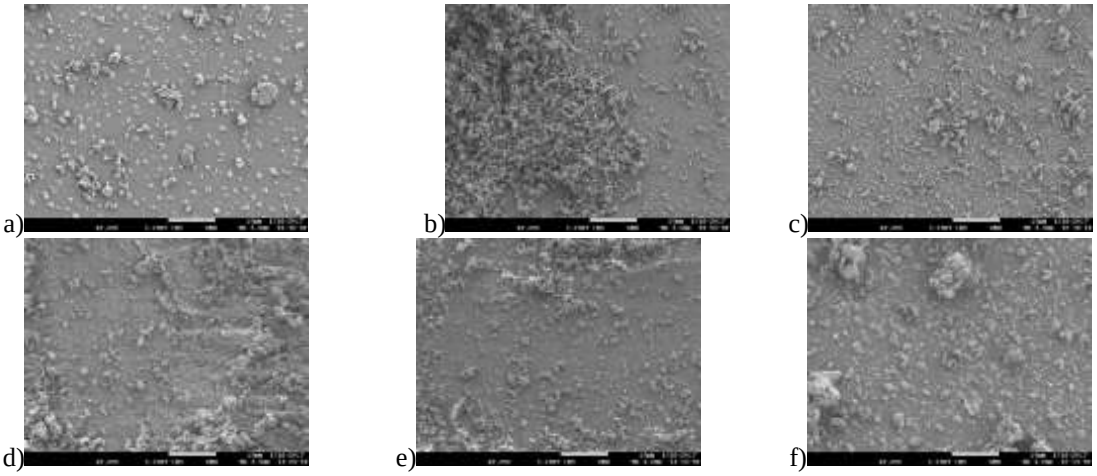

Figure 4: Composites of a) TiO_2-Eri (25-75), b)TiO_2-Cli (25-75), c)TiO2-Mor (25-75), d)TiO_2-Eri (75-25), e)TiO_2-Cli (75-25) y f)TiO_2-Mor (75-25).

IV. CONCLUSIONS

Thanks to the characterization of XRD it was possible to distinguish the presence of crystalline phases in the films of the TiO_2-Zeolite compounds, whereas in RAMAN it was possible to appreciate two vibration

modes related to the anatase phase of TiO_2, while in UV- Vis it was possible to determine the band gap of TiO_2 Zeolite films ranging between 4.03-4.46 eV for films of TiO_2-Zeolite composites, when compared with previous studies, an increase in band interval, such time due to the fact that the films have a reduction of the crystallographic orientations which generates an increase in the conductivity, finally, we can observe the different morphologies that these films present.

ACKNOWLEDGEMENTS

The authors would like to acknowledge the financial support to CONACyT con el numero de proyecto366748, as well as to the financial support from the RCUK-CONACYT project and Proyecto VIEP No. 486

REFERENCES

[1]. T. K. Tseng, Y. S. Lin, Y. J. Chen and H. Chu., A Reviem of Photocatalysts Prepares by Sol-Gel Method for VOCs Removal. Int. J. Mol. Sci. 11 (2010), p.p. 2336-2361. doi:10.3390/ijms11062336

[2]. G. Zhang, A. Song, Y. Duan and S. Zheng., Enhanced photocatalytic activity of TiO2_zeolite composite for abatement of pollutants. Microporous and Mesoporous Materials. 255 (2018), p.p. 61-68.https://doi.org/10.1016/j.micromeso.2017.07.028

[3]. S. M. Hosseini, S. H. Amini, A. R. Khodabakhshi, E. Bagheripour and B. Van der Bruggen., Activated carbon nanoparticles entrapped mixed matrix polyethersulfone based nanofiltration membrane for sulfate and copper removal from water. Journal of the Taiwan Institute of Chemical Engineers. 82 (2018), p.p. 169-178.https://doi.org/10.1016/j.jtice.2017.11.017

[4]. A. Zielinska, M. Klein and J. Hupka., Enhanced visible light photocatalytic activity of Pt/I-TiO2 in a slurry system and supported on glass packing. Separation and Purification Technology.189 (2017) p.p. 246-252. https://doi.org/10.1016/j.seppur.2017.08.018.

[5]. K. Deepak Kumar, G. Praveen Kumar and K. Srinivasulu Reddy., Rapid Microwave Synthesis of Reduced Graphene Oxide-supported TiO2 Nanostructures as High Performance Photocatalyst. Materials Today Proceedings. 2 (2015) p.p. 3736-3742.https://doi.org/10.1016/j.matpr.2015.07.204.

[6]. C. Wang, H. Shi and Y. Li., Synthesis and characteristics of natural zeolite supported Fe^{3+} -TiO_2 Photocatalysts. Applied Surface Science. 257 (2011) p.p. 6873-6877.https://doi.org/10.1016/j.apsusc.2011.03.021

[7]. X. Liu, Y. Liu, S. Lu, W. Guo and B. Xi., Performance and mechanism into TiO_2/Zeolite composites for sulfadiazine adsorption and photodegradation. Chemical Engineering Journal. 350 (2018) p.p. 131-147.https://doi.org/10.1016/j.cej.2018.05.141

[8]. I. Jansson, S. Suárez, F. J. Garcia-Garcia and B. Sánchez. Zeolite-TiO_2 hybrid composites for pollutant degradation in gas phase. Applied Catalysis B: Enviromental. 178 (2015) p.p. 100-107.https://doi.org/10.1016/j.apcatb.2014.10.022

[9]. E. Mansoor, J. Van der Mynsbrugge, M. Head-Gordon and A. T. Bell. Impact of long-range electrostatic and dispersive interactions on theoretical predictions of adsorption and catalysis in zeolite. Catalysis Today. 312 (2018) p.p. 51-65.https://doi.org/10.1016/j.cattod.2018.02.007

[10]. A. Feliczak-Guzik., Hierarchical zeolites: Synthesis and catalytic properties. Microporous and Mesoporous Materials. 259 (2018) p.p. 33-45.https://doi.org/10.1016/j.micromeso.2017.09.030

[11]. L. B. McCusker, F. Liebau and G. Engelhardt. Nomenclature of structural and compositional characteristics of ordered microporous and mesoporous materials with inorganic hosts (IUPAC redommend 2001). Mircoporous and Mesoporous Materials. 58 (2003) p.p. 3-13.

[12]. M. Richter, K. Ehrhardt, U. Roost, H. Kosslick and B. Parlitz., Molecular sieving of n-butanes by zeolite erionite and by isostructuralsilicoaluminophosphate SAPO-17. Studies in Surface Science and Catalysis. 84 (1994) p.p. 1285-1292.https://doi.org/10.1016/S0167-2991(08)63669-1

[13]. M. Fujiwara, T. Kitabayashi, K. Shiokawa and T. K. Moriuchi., Sealing and reopening of micropores of mordenite and ZSM-5 by disilylbenzene compounds. Microporous and Mesoporous Materials. 115 (2008) p.p. 556-561.https://doi.org/10.1016/j.micromeso.2008.02.034

[14]. D. A. Kennedy and F. H. Tezel., Cationexchande modification of clinoptilolite – Screaning analysis for potential equilibrium and kinetic adsorption separations involving methane, nitrogen, and carbon dioxide. Microporous and Mesoporous Materials. 262 (2018) p.p. 235-250.https://doi.org/10.1016/j.micromeso.2017.11.054

[15]. K. M. Alvarez, J. Alvarado, B. S. Soto and M. A. Hernandez., Synthesis of TiO_2 nanoparticles and TiO_2-Zeolite composite and study of optical properties and structural characterization. Optik. 169 (2018) p.p. 137-146. https://doi.org/10.1016/j.ijleo.2018.05.028

[16]. K. Quiroz, M. A. Hernández, R. Portillo, F. Rojas, E. Rubio, V. Petranovskii. *Superficies y Vacío.*.29, 55 (2016). http://smctsm.org.mx/ojs/index.php/SyV/article/view/41/36

[17]. F. Y. Cui, A. Kundu, A. Krause, M. P. Harmer and R. P. Vinci. Surface energies, segregation, and fracture behavior of magnesium aluminate spinel low-index grain boundary planes. ActaMaterialia. 148 (2018) p.p. 320-329.https://doi.org/10.1016/j.actamat.2018.01.039

[18]. S. de Almeida-Didry, C. Autret, C. Honstettre, A. Lucas, M. Zaghrioui, F. Pacreau and F. Gervais., Central role of TiO_2anatase grain boundaries on resistivity of $CaCu_3Ti_4O_{12}$-based materials probed by Raman spectroscopy. Solid State Sciences 61 (2016) p.p. 102-105.https://doi.org/10.1016/j.solidstatesciences.2016.07.010

[19]. H. M. Ali, E. M. M. Ibrahim, M. M. Wakkad and M. A. A. Mohamed., Effect of the synthesis conditions on the structural, morphological and optical properties of $Bi_2Te_{2.7}Se_{0.3}$ nanoparticles. Optik 158 (2018) p.p. 199-203.https://doi.org/10.1016/j.ijleo.2017.12.090

[20]. R. Gerdes, H. Betterntrup, D. Enseling, M. Haase and T. Jüstel., On the synthesis, phase optimisation and luminescence of some rare earth pyrosilicates. Journal of Luminescence 190 (2017) p.p. 451-456. https://doi.org/10.1016/j.jlumin.2017.06.001

[21]. W. Zhi-Ming, X. Qing-Yu, Z. Shi-Yuan, X. Ding-Yu and D. You-Wei. Difference in electric conduction of monocrystal and polycrystal graphite. Chin. Phys. Soc. 56 (2007) p.p. 3464-3467. http://www.oalib.com/paper/1444385#.W8ztY1VKjIU

K. M. Álvarez "Structural and optical properties of TiO2 and TiO2-Zeolites composites films "International Journal Of Engineering Research And Development , vol. 14, no. 09, 2018, pp. 43-49